Modelling of Anisotropic Synchronous Machine in Stator Reference Frame

Jie Fang, Carsten Heising, Volker Staudt and Andreas Steimel
Ruhr-University Bochum
D-44780 Bochum
Germany
Tel.: +49 234 32 23890
Fax.: +49 234 32 14597
Email: fang@eele.rub.de, heising@eele.rub.de, staudt@eele.rub.de, steimel@eele.rub.de

***Abstract*—Interior permanent magnet-synchronous machines (IPMSM) feature many favourable properties for e-mobility application as high power density and good efficiency. However, they require careful modelling because of strong anisotropies of the rotor, as they are also known from salient-pole synchronous machines. These anisotropies are often accounted for by different values for the d-axis and q-axis inductances in a rotor-flux-oriented coordinate system. With regard to asynchonous machine control, stator-flux-oriented control could provide improved dynamic behaviour – especially in the field-weakening range. The representation of fault conditions inside the machine, leading to asymmetrical machine parameters, suggests a phase-wise description instead of the usual two-axis (d-q or space-vector) analysis.**

This paper presents a machine model which provides a basis for stator-flux-oriented control and for the simulation of fault conditions inside the machine. This is reached by a phase-wise representation based on the known approach using rotor-flux-oriented d-axis and q-axis inductances. A physical interpretation for self and mutual inductances is given. A single-phase winding interruption fault is simulated to outline the capability of the chosen approach.

I. Introduction

Modelling of salient-pole synchronous machines and permanent-magnet synchronous machines (PMSM) – usually with interior magnets (IPMSM) – with anisotropic characteristics is usually based on a rotor-flux-oriented coordinate system employing different values for the d-axis and q-axis inductances L_d and L_q. Such a model can only represent symmetrical machines. In case of faults inside the machine, for example a single-phase winding interruption or partial short, asymmetries result. Accordingly the relevant machine parameters become asymmetrical and can no longer be represented by the L_d-L_q two-axis model. In such a case a phase-wise model is necessary. For isotropic induction machines such a phase-wise representation is described in [1], [2]. This model allows to simulate any unsymmetrical fault condition inside isotropical induction machines if the influence of the fault condition on the machine parameters is known.

To include the influence of anisotropies the method has to be extended. For this purpose, the typical rotor-flux oriented L_d-L_q model of anisotropy is transformed into the stator-fixed reference frame. Subsequently, an inverse space-vector transformation is performed, leading to the desired model. The resulting differential equations meet the requirements stated above – simulation studies for synchronous machines with anisotropies under asymetrical faults inside the machine can be performed.

Please note that the same methodology applies for IPMSM and salient-pole synchronous machines – in the first case, mainly $L_d < L_q$ applies, in the second case $L_d > L_q$. In the following salient-pole machines are used as representation of both types of machine without causing any restrictions.

Simulation results are given, e.g. for a single-phase machine-winding interruption fault, to demonstrate the capability of the introduced model. The simulator is employed completely implemented in C code and optimized for power-electronic systems [3]–[5].

II. Flux-linkage equations of a synchronous machine without damper winding

The flux linkage in the synchronous machines can be expressed in rotor-flux oriented (d-q) space-vector form. The d-axis is defined by the rotor structure (cp. Fig. 1) [6]:

$$\Psi_d = L_d i_d + \Psi_{rotor} = (L_{hd} + L_\sigma)\, i_d + \Psi_{rotor} \quad (1)$$

$$\Psi_q = L_q i_q = (L_{hq} + L_\sigma)\, i_q \quad (2)$$

In the case of salient-pole machines, Ψ_{rotor} will be expressed by $L_E \cdot i_E$, where L_E and i_E are the exciter inductance and the exciter current of rotor. In the case of PMSM, Ψ_{rotor} is the remanence flux of the permanent magnet. In the following, only the salient-pole machines will be used as represntation.

On the other hand the phase quantities of the flux linkages can be represented by:

$$\Psi_a = L_{aa} i_a + L_{ab} i_b + L_{ac} i_c + \Psi_{a,rotor} \quad (3)$$

$$\Psi_b = L_{ba} i_a + L_{bb} i_b + L_{bc} i_c + \Psi_{b,rotor} \quad (4)$$

$$\Psi_c = L_{ca} i_a + L_{cb} i_b + L_{cc} i_c + \Psi_{c,rotor} \quad (5)$$

where $\Psi_{i,rotor}$ $(i = a, b, c)$ describe the reactions between the windings of stator and rotor, the maximal value of $\Psi_{i,rotor}$ will be achieved, when the i- and d-axis have the same direction [7]. L_{ij} is the mutual inductance (for $i \neq j$) or the self

978-1-4244-8218-4/10/$26.00 ©2010 IEEE

inductance (for $i = j$), which describe the winding-winding-reactions (cp. Fig. 2, 3).

A direct identification of all parameters with their dependencies on L_d and L_q is rather complicated. This problem can be simplified considerably and solved easily by reversing the process. The starting point is the L_d-L_q model. A transformation of the model into phase quantities applying an inverse space-vector transformation follows. Finally, a comparison of coefficients is carried out. Subsequently, the respective inductivities can be determined as functions of L_d, L_q and rotor position angle χ.

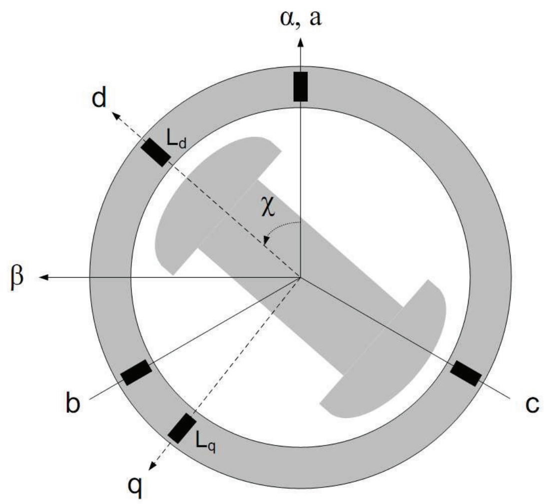

Fig. 1. Synchronous salient-pole machine without damper winding - equivalent windings and their position

III. Coordinate transformation

The transformation is carried out in two steps. At first, the d- and q- components of the currents, i_d and i_q in (1) and (2) are replaced by the phase quantities i_a, i_b and i_c:

$$i_d = i_\alpha \cos\chi + i_\beta \sin\chi \tag{6}$$
$$i_q = i_\beta \cos\chi - i_\alpha \sin\chi \tag{7}$$
$$i_\alpha = \frac{2}{3} i_a - \frac{1}{3} i_b - \frac{1}{3} i_c \tag{8}$$
$$i_\beta = \frac{1}{\sqrt{3}} i_b - \frac{1}{\sqrt{3}} i_c \tag{9}$$

The current components i_d and i_q are calculated as follows:

$$i_d = \frac{1}{3}\left\{(2i_a - i_b - i_c)\cos\chi + \sqrt{3}\,(i_b - i_c)\sin\chi\right\} \tag{10}$$
$$i_q = \frac{1}{3}\left\{\sqrt{3}\,(i_b - i_c)\cos\chi + (-2i_a + i_b + i_c)\sin\chi\right\} \tag{11}$$

The equations above are inserted into equations 1 und 2. Subsequently, the d, q-components of flux are converted into phase quantities:

$$\Psi_\alpha = \Psi_d \cos\chi - \Psi_q \sin\chi \tag{12}$$
$$\Psi_\beta = \Psi_d \sin\chi + \Psi_q \cos\chi \tag{13}$$
$$\Psi_a = \Psi_\alpha \tag{14}$$
$$\Psi_b = -\frac{\Psi_\alpha}{2} + \frac{\sqrt{3}}{2}\Psi_\beta \tag{15}$$
$$\Psi_c = -\frac{\Psi_\alpha}{2} - \frac{\sqrt{3}}{2}\Psi_\beta \tag{16}$$

With the computations above, the phase quantities of the fluxes $\Psi_{a,b,c}$ result in

$$\begin{aligned}\Psi_a = {} & \frac{2}{3}\left(L_{hd}\cos^2\chi + L_{hq}\sin^2\chi\right) i_a \\ & + \frac{1}{3}\left(\sqrt{3}(L_{hd} - L_{hq})\sin\chi\cos\chi - L_{hd}\cos^2\chi - L_{hq}\sin^2\chi\right) i_b \\ & + \frac{1}{3}\left(\sqrt{3}(L_{hq} - L_{hd})\sin\chi\cos\chi - L_{hd}\cos^2\chi - L_{hq}\sin^2\chi\right) i_c \\ & + \Psi_{rotor}\cos\chi + \underbrace{L_{\sigma a}\left(2i_a/3 - i_b/3 - i_c/3\right)}_{L_{\sigma a} i_a}\end{aligned} \tag{17}$$

$$\begin{aligned}\Psi_b = {} & \frac{1}{3}\left(\sqrt{3}\sin\chi\cos\chi(L_{hd} - L_{hq}) - L_{hd}\cos^2\chi - L_{hq}\sin^2\chi\right) i_a \\ & + \frac{1}{6}\left(2(L_{hd} + L_{hq}) - (L_{hd} - L_{hq})\left(\sqrt{3}\sin 2\chi + \cos 2\chi\right)\right) i_b \\ & + \frac{1}{6}(2(L_{hd} - L_{hq})\cos 2\chi - L_{hd} - L_{hq}) i_c \\ & + \Psi_{rotor}\cos(\chi - 120^\circ) + \underbrace{L_{\sigma b}\left(-i_a/3 + 2i_b/3 - i_c/3\right)}_{L_{\sigma b} i_b}\end{aligned} \tag{18}$$

$$\begin{aligned}\Psi_c = {} & \frac{1}{3}\left(\sqrt{3}(L_{hq} - L_{hd})\sin\chi\cos\chi - L_{hd}\cos^2\chi - L_{hq}\sin^2\chi\right) i_a \\ & + \frac{1}{6}(2(L_{hd} - L_{hq})\cos 2\chi - L_{hd} - L_{hq}) i_b \\ & + \frac{1}{6}\left((L_{hd} - L_{hq})\left(\sqrt{3}\sin 2\chi - \cos 2\chi\right) + 2(L_{hd} + L_{hq})\right) i_c \\ & + \Psi_{rotor}\cos(\chi - 240^\circ) + \underbrace{L_{\sigma c}\left(-i_a/3 - i_b/3 + 2i_c/3\right)}_{L_{\sigma c} i_c}\end{aligned} \tag{19}$$

All inductivities can be determined by comparing the equations (3), (4) and (5) with the equations (17), (18) und (19).

$$\begin{aligned} L_{aa} &= \frac{2}{3}\left(L_{hd}\cos^2\chi + L_{hq}\sin^2\chi\right) + L_{\sigma a} \\ L_{bb} &= \frac{1}{6}\left(2(L_{hd} + L_{hq}) - (L_{hd} - L_{hq})\left(\sqrt{3}\sin 2\chi + \cos 2\chi\right)\right) + L_{\sigma b} \\ L_{cc} &= \frac{1}{6}\left((L_{hd} - L_{hq})\left(\sqrt{3}\sin 2\chi - \cos 2\chi\right) + 2(L_{hd} + L_{hq})\right) + L_{\sigma c} \\ L_{ab} &= \frac{1}{3}\left(\sqrt{3}(L_{hd} - L_{hq})\sin\chi\cos\chi - L_{hd}\cos^2\chi - L_{hq}\sin^2\chi\right) \\ L_{ac} &= \frac{1}{3}\left(\sqrt{3}(L_{hq} - L_{hd})\sin\chi\cos\chi - L_{hd}\cos^2\chi - L_{hq}\sin^2\chi\right) \\ L_{bc} &= \frac{1}{6}(2(L_{hd} - L_{hq})\cos 2\chi - L_{hd} - L_{hq}) \\ L_{ab} &= L_{ba} \\ L_{ac} &= L_{ca} \\ L_{bc} &= L_{cb} \end{aligned} \tag{20}$$

Please note that the position-dependent three self inductances and the three mutual inductances have portions oscillating with 2χ and phase-shifted by 120° (see Fig. 2 bottom).

It can be mathematically shown that all the self-inductances are given by the following term:

$$
\begin{aligned}
L_{aa} &= \frac{1}{3}\left[(L_{hd}+L_{hq})+(L_{hd}-L_{hq})\cos 2\chi\right]+L_{\sigma a}\\
L_{bb} &= \frac{1}{3}\left[(L_{hd}+L_{hq})+(L_{hd}-L_{hq})\cos\left(2\chi+120^{\circ}\right)\right]+L_{\sigma b}\\
L_{cc} &= \frac{1}{3}\left[(L_{hd}+L_{hq})+(L_{hd}-L_{hq})\cos\left(2\chi+240^{\circ}\right)\right]+L_{\sigma c}
\end{aligned} \tag{21}
$$

The same applies to the mutual inductances and the magnetic flux components of the rotor:

$$
\begin{aligned}
L_{bc} &= \frac{1}{3}\left[-\frac{(L_{hd}+L_{hq})}{2}+(L_{hd}-L_{hq})\cos\left(2\chi\right)\right]\\
L_{ab} &= \frac{1}{3}\left[-\frac{(L_{hd}+L_{hq})}{2}+(L_{hd}-L_{hq})\cos\left(2\chi-120^{\circ}\right)\right]\\
L_{ac} &= \frac{1}{3}\left[-\frac{(L_{hd}+L_{hq})}{2}+(L_{hd}-L_{hq})\cos\left(2\chi-240^{\circ}\right)\right]\\
\Psi_{a,rotor} &= \Psi_{rotor}\cos\left(\chi-0^{\circ}\right)\\
\Psi_{b,rotor} &= \Psi_{rotor}\cos\left(\chi-120^{\circ}\right)\\
\Psi_{c,rotor} &= \Psi_{rotor}\cos\left(\chi-240^{\circ}\right)
\end{aligned} \tag{22}
$$

IV. The physical interpretation of the inductances and the related angle dependency χ

For deriving the voltage equations for all phases, the physical meaning of selfinductance and mutualinductance in context of anisotropies is analysed. The equations (21) und (22) represent the influence of the air-gap distance varying with angle χ.

The inductivities of the self and the mutual inductances change with twice the frequency of the mechanical rotation of the rotor times the number of pole pairs. This can be explained by a closer look at geometrical issues. For reduction of complexity, the number of pole pairs is assumed to be one.

Because of identical geometry, the same air-gap distance is found for $\chi = 0^{\circ}$ and $\chi = 180^{\circ}$. At $\chi = 0^{\circ}$ the selfinductance L_{aa} is maximal because the air gap underneath the winding a is minimal (see Fig. 2 top left). For the mutual inductance L_{bc}, the airgap between windings b and c is as large as possible. In consequence, the mutual inductance L_{bc} is minimal.

If the rotor is rotated by 90°, the situation reverses: The air gap underneath winding a is as large as possible. Therefore, L_{aa} has minimal value. The air gap between windings b und c, however, is as small as possible. Consequently, the inductivity of the mutual inductance is maximal (see Fig. 2 top right).

V. Fault simulation using voltage equations for a three-phase salient-pole synchronous machine

Using the basic differential equation describing an inductance, the voltage equations for the three stator windings can be given. For this, the equations (21) and (22) are inserted into equations (3) to (5).

$$
\begin{aligned}
u_a &= r_a i_a + \frac{d\left(L_{aa}i_a\right)}{dt}+\frac{d\left(L_{ab}i_b\right)}{dt}+\frac{d\left(L_{ac}i_c\right)}{dt}+\frac{d\left(\Psi_{a,rotor}\right)}{dt}\\
u_b &= r_b i_b + \frac{d\left(L_{ba}i_a\right)}{dt}+\frac{d\left(L_{bb}i_b\right)}{dt}+\frac{d\left(L_{bc}i_c\right)}{dt}+\frac{d\left(\Psi_{b,rotor}\right)}{dt}\\
u_c &= r_c i_c + \frac{d\left(L_{ca}i_a\right)}{dt}+\frac{d\left(L_{cb}i_b\right)}{dt}+\frac{d\left(L_{cc}i_c\right)}{dt}+\frac{d\left(\Psi_{c,rotor}\right)}{dt}
\end{aligned} \tag{23}
$$

According to the equations, an equivalent electric circuit can be deduced (cp. Fig. 3). The reference of the three stator voltages u_a, u_b and u_c is u_0. The stator-winding resistances and the leakage-inductances do not depend on the rotor positon χ. The equations (23) can be used to simulate different operation points, both in normal operation and in failure operation – for example: in case of sudden interruption of a single phase winding. As stated before, the simulation of such a fault condition is impossible with the normal L_d–L_q model.

In the following, the deduced model of a converter-fed salient-pole SM (with $L_d > L_q$) is applied under different conditions, in order to outline the capability. In all scenarios, the SM is operated with fixed synchronous speed due to the fact that the electrical behaviour shall be assessed. The machine parameters, which was used in the simulator, is shown in the Table I.

TABLE I
PARAMETERS OF THE SIMULATION

L_d	0.03 H
L_q	0.02 H
$\Psi_{rotor} = L_E \cdot i_E$	0.6 Vs
$L_{\sigma a,b,c}$ initial	0.001 H
$L_{\sigma a}$ by construction fault	0.002 H
$r_{a,b,c}$ initial	0.062 Ω
r_a by interruption	10 kΩ
DC-link voltage	700 V
switching frequency of the three-phase inverter	1250 Hz

There were three scenarios simulated. In scenario 1 (see Fig. 4) the SM is in normal operation. All three stator currents are symmetrical due to the symmetrically chosen machine parameters.

In the scenario 2 (see Fig. 5) the phase a is assumed to be interrupted at instant $t = 4\,\mathrm{s}$, when the resistance of stator winding r_a is set to $10\,\mathrm{k\Omega}$ (cp. Fig. 4), modelling an interruption of the winding. The current i_a quickly decreases to zero. The other two phase currents are not shifted by 120° any longer, following immediately from Kirchhoff's Current Law $i_b = -i_c$). After the interruption of phase a the amplitude of the phase b and c decrease to $\sqrt{3}/2$.

In the scenario 3 (see Fig. 6) phase a is assumed to have big leakage inductance related to e.g. a construction fault; it is set to two times the leakage inductances of the other phases. Due to this fault the phase-current i_a is smaller compared to the other phase currents.

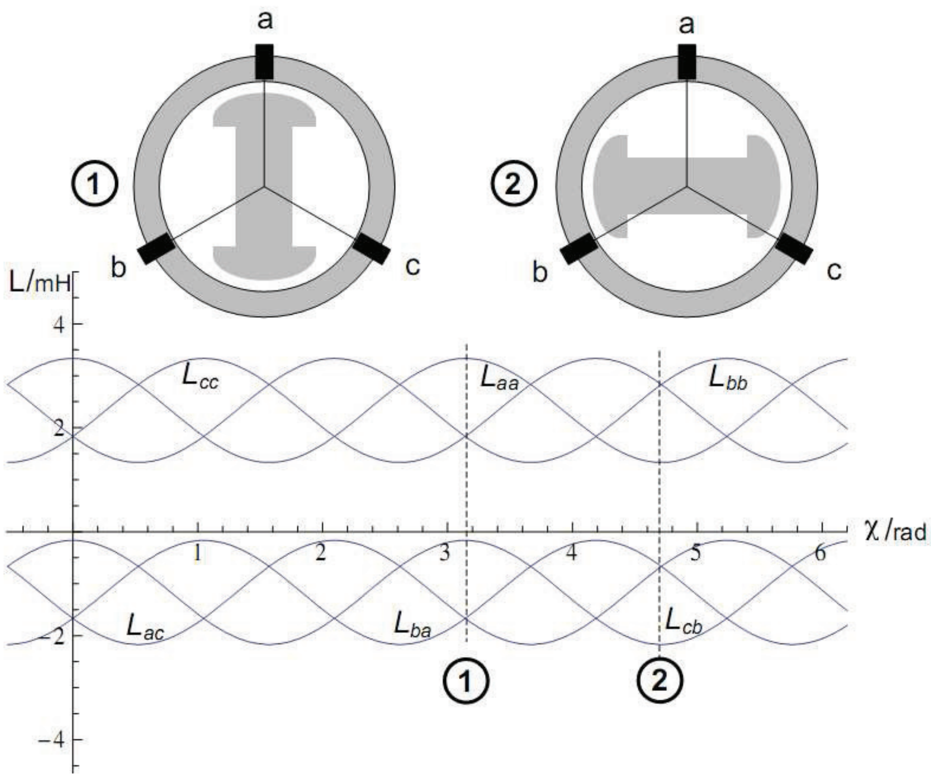

Fig. 2. Variation of the self inductance and the mutual inductance with the rotor angle χ

.

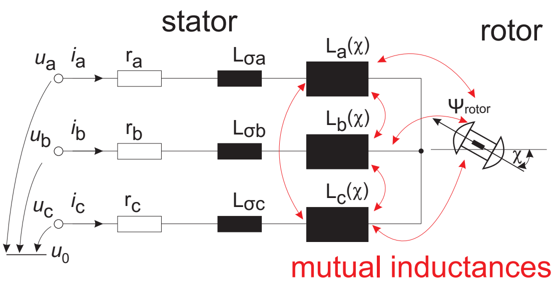

Fig. 3. The equivalent electric circuit of a salient-pole synchronous machine

VI. CONCLUSION

This paper presents a stator-oriented phase-wise model of a synchronous machines. The synchronous machine may be anisotropic and asymmetric. Anisotropies usually result from salient-pole or interior permanent-magnet characteristics, asymmetries from fault conditions inside the machine. The model allows the simulation of unsymmetrical fault inside the machine, e.g. single phase-winding interruptions, for anisotropic machines.

The differential equations and their parameters are derived for the stator-oriented reference frame. The basis are the commonly known d-axis and q-axis inductances L_d and L_q, defined in a rotor-flux-oriented coordinate system. A physical interpretation of the variation of self and mutual inductances with the position angle of the rotor is given.

The capability of the approach to represent asymmetrical machine-side faults for anisotropic machines is illustrated by simulation results of different scenarios. The reaction of control schemes to such faults can be analysed. The model described is intended to enable the development of advanced stator-flux oriented control schemes, being robust to asymmetrical faults.

REFERENCES

[1] C. Heising, M. Oettmeier, R. Bartelt, J. Fang, V. Staudt, and A. Steimel, "Modelling method for complex induction machines used in naval applications using an advanced simulation concept," in *IEEE Electric Ship Technologies Symposium (ESTS)*, (Baltimore, Maryland/USA), pp. 278 – 281, 2009.

[2] C. Heising, M. Oettmeier, R. Bartelt, F. Jie, V. Staudt, and A. Steimel, "Simulation of asymmetric faults of a five-phase induction machine used in naval applications," in *35th Annual Conference of the IEEE Industrial Electronics Society (IECON)*, (Porto, Portugal), 2009.

[3] C. Heising, M. Oettmeier, R. Bartelt, V. Staudt, and A. Steimel, "Advanced simulation concept for onboard ship grids featuring complex multiterminal power-electronic systems," in *IEEE Electric Ship Technologies Symposium (ESTS)*, (Baltimore, Maryland/USA), pp. 170 – 173, 2009.

[4] R. Bartelt, C. Heising, M. Oettmeier, V. Staudt, and A. Steimel, "Advanced simulation concept for power electronic systems applied to the 3-level npc inverter," in *35th Annual Conference of the IEEE Industrial Electronics Society (IECON)*, (Porto, Portugal), 2009.

[5] V. Staudt, C. Heising, and A. Steimel, "Advanced simulation concept for power train of loco and its verification," in *ICPE 07 Conference*, (Daegu, South Korea), 2007.

[6] D. Schroeder, *Elektrische Antriebe - Regelung von Antriebssystemen, 3. Auflage*. Springer-Verlag Berlin-Heidelberg, 2009.

[7] G. Mueller, *Elektriche Maschinen*. VEB VERLAG TECHNIK BERLIN, 1966.

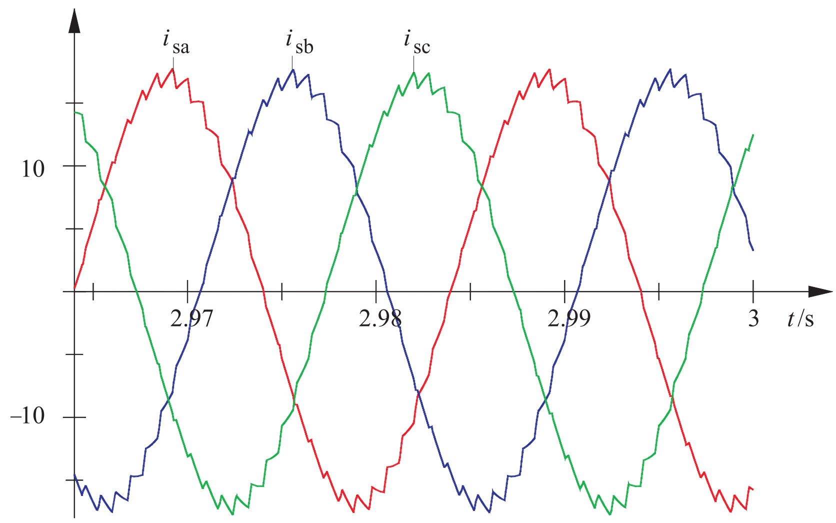

Fig. 4. Stator currents of salient-pole SM in normal operation point, red: i_{sa}, blue: i_{sb}, green: i_{sc}.

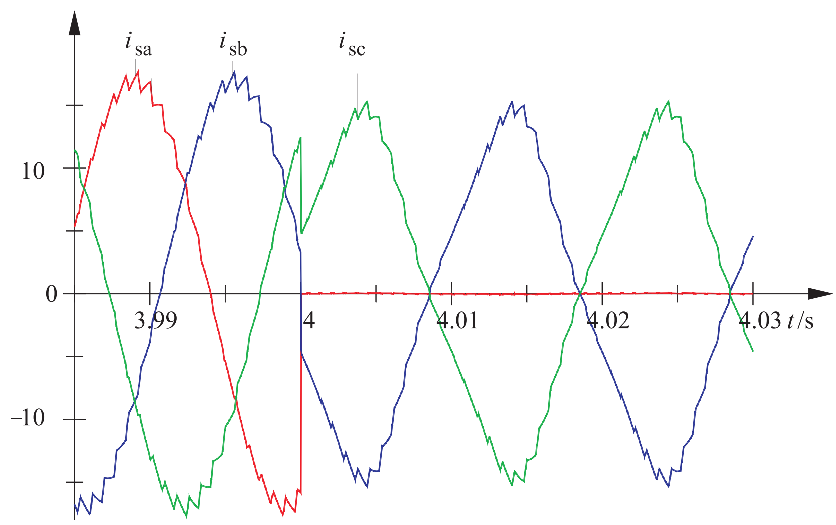

Fig. 5. Stator currents of salient-pole SM, interruption of winding at $t = 4\,\mathrm{s}$ $r_a = 10\,\mathrm{k\Omega}$, red: i_{sa}, blue: i_{sb}, green: i_{sc}.

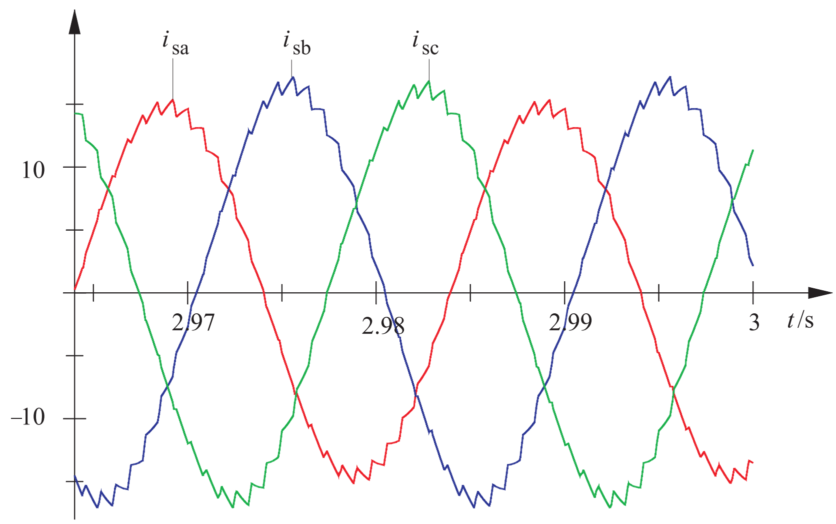

Fig. 6. Construction fault in phase a of salient-pole SM, red: i_{sa}, blue: i_{sb}, green: i_{sc}.